Journal of Geomatics Vol 9 No. 1April 2015

Comparing modelled Arctic sea ice trend with remotely sensed estimates

D. Ram Rajak, Neeraj Agarwal, P. Jayaprasad,
R.K. Kamaljit Singh, Sandip R. Oza and Rashmi Sharma
Ocean Sciences Division, AOSG/EPSA
Space Applications Centre (ISRO), Ahmedabad – 380015, India.
Email: rajakdr@sac.isro.gov.in

(Received: Dec 24, 2014; in final form: Mar 25, 2015)

Abstract: To assess the appropriateness of Massachusetts Institute of Technology global ocean circulation model (MITgcm) derived sea ice, monthly average Sea Ice Area (SIA) derived from modelled Sea Ice Concentration (SIC) has been compared with satellite derived SIA (NSIDC/NASATEAM sea ice area) in Arctic region. MITgcm coupled to a thermodynamic sea-ice model has been used. Data from 1980 to 2010 has been used for comparison. The model domain is global and the zonal grid spacing is 1° longitude, while the meridional ocean grid spacing is 0.3° of latitude within 10° of the Equator increasing to 1° latitude pole-ward of 22°N and 22°S. It was found that the overall sea ice spatial and temporal variations in Arctic region were simulated well by the model. The simulated sea ice area trends were quite similar to satellite derived sea ice area trends. Model overestimated the rate of decrease of sea ice area when compared to satellite derived sea ice area. Modelled rate of decrease was 3.7% in comparison to satellite based rate of 1.8% over the period of 31 years (1980 to 2010). An important observation was that satellite derived SIA initially increased during 1979 to 1992 time period by 5.4% followed by a reduction of 6.8% between 1993 and 2013 time period. Overall, a decrease of almost 2.3% has been observed from 1979 to 2013.

Keywords: Sea ice area, Arctic, MITgcm, Sea ice trend

1. Introduction

Ice in the sea has major two origins: the freezing of seawater and the ice broken off from glaciers. Frozen seawater is called sea ice. The density of sea ice is less than water; hence it always floats on ocean water. About 7% of the area of the world ocean which is approximately 30 million km^2 is comprised of sea ice. In the Northern hemisphere maximum sea-ice occurs during March when entire Arctic ocean and adjoining seas are frozen while the minima occurs in September and the sea-ice is confined to the Arctic ocean, Greenland seas and the Canadian archipelago. Opposite to Northern hemisphere, in the Southern hemisphere the minimum occurs in February while the maxima occurs in September when the Antarctic continent is surrounded by ice and extends up-to 60-55^o S (Gloersen et al., 1992).

Sea-ice monitoring is of enormous importance both climatically and also for navigation purposes in higher latitudes. It interposes an insulating layer between the ocean and the atmosphere restricting the exchange of heat, freshwater and momentum fluxes between the two. Melting and formation of sea-ice modifies the air-sea interaction and ocean atmosphere feedback processes. When the ocean is covered by sea-ice then due to high albedo of sea-ice the solar radiation incident gets reflected back to the atmosphere resulting in very less heat absorption by the surface. On the other hand when the sea-ice melts, the ocean underneath exposes and due to low albedo of the ocean, solar radiation is absorbed resulting in net heating of the ocean. This affects the net heat transferred to/from the ocean and hence influences the global heat budget. This is most significant in summer when the solar heating is higher.

Additionally, sea ice provides an ecosystem for various polar species, particularly the polar bear in Arctic, whose environment is being threatened due to enhanced melting of ice (including sea ice in Arctic region). Hence it is very important to continuously monitor and predict sea-ice, mainly to monitor environment, specifically climate change.

Now-a-days, sea ice record prepared based on satellite data include sea ice extent, area, concentration, thickness and the age of the sea ice. Sea ice in Antarctic region is very different than in Arctic region as far as its age, thickness, growth/melting patterns, snow coverage etc. are concerned. Based on analysis of 10 years data, Massom et al., 2001 found large regional and seasonal differences in snow properties and thicknesses and consequences of thicker snow and thinner ice in the Antarctic relative to the Arctic.

Most of the satellite derived Sea Ice Concentration (SIC) products available till date are derived using passive microwave techniques, e.g., Bootstrap algorithm (Comiso, 1986, 1995), NASA Team (NT) Algorithm (formerly, Nimbus-7 Team algorithm) (Cavalieri et al., 1984), NT2 (Markus and Cavalieri, 2000), Arctic Radiation and Turbulence Interaction STudy (ARTIST) Sea Ice (ASI) (Kaleschke et al.., 2001; Spreen et al., 2008), Ocean Sea Ice (OSI) algorithm (Breivik et al., 2014). QuikSCAT data were used for the correction of ice classification (Walker et al., 2006; Shalina and Johannesen, 2008). Oza et al., 2010 investigated sea ice trend at $1^o \times 1^o$ grid level over 2000–2007 period using QuikSCAT scatterometer data

and found that overall monthly trend was negative in all the Arctic sectors. Zwally et al., 2008 derived sea ice freeboard heights in the Weddell Sea of Antarctica from ICESat (Ice, Cloud, and Land Elevation Satellite) laser altimeter measurements.

To begin with simulations, the earliest ice models were energy balance models (Budyko, 1969; Sellers, 1969) which mainly accounted for ice albedo feedback by parameterizing ocean surface albedo as a function of sea surface temperature. Hibler (1979, 1980) developed the numerical treatment of ice as a viscous-plastic (VP) material and also explicitly modelled the ice-thickness distribution. This was followed by elastic-viscous-plastic (EVP) model proposed by Hunke and Dukowicz (1997). These new dynamical schemes evolved in a time of rapid improvement in the sea ice dynamics in climate models, and now EVP and VP dynamics are in wide use among climate models. Similarly sea-ice thermodynamic models also evolved starting with the thermodynamic model of Maykut and Untersteiner (1971) which was improved to include brine pockets by Bitz and Lipscomb (1999).

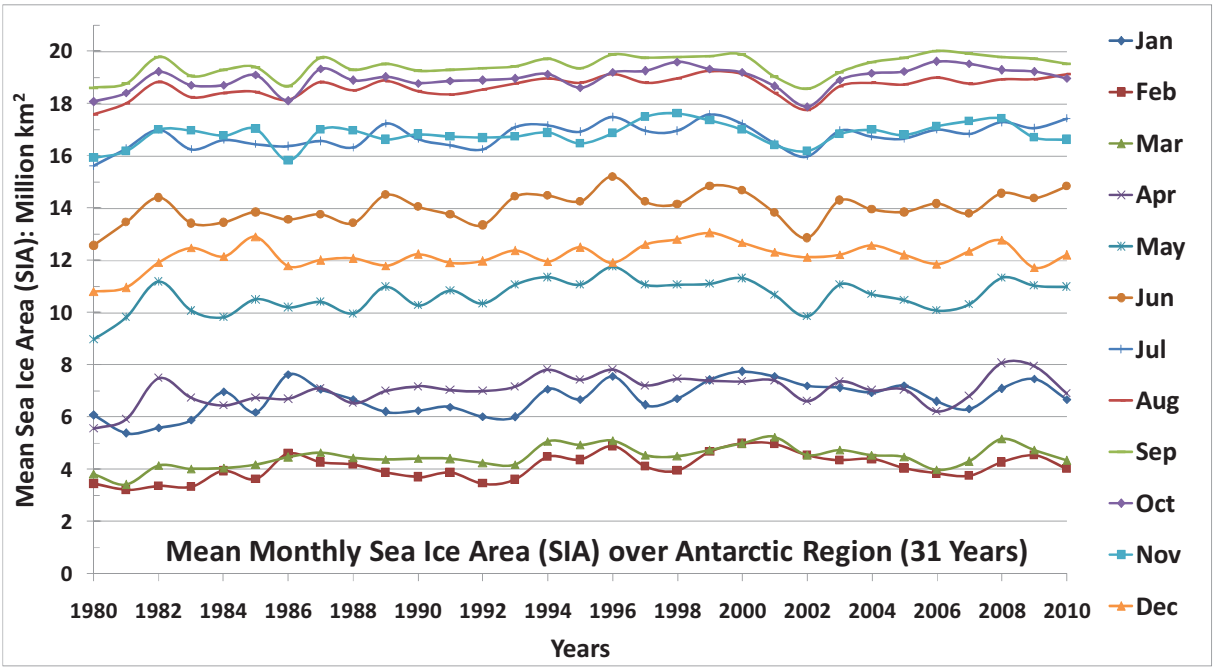

Figure 1: Variation of MSMMSIA over Arctic region

Several sensitivity studies have been performed using numerical models including the effects of surface precipitation (Powell et al., 2005), winds (Stossel et al., 2011) and ice-shelf melt-water (Hellmer, 2004). Models have also been used to assess linkages between sea ice variability and large-scale climate modes (Lefebvre and Goosse, 2005, 2008). Several such models have been validated against ice observations, including those of ice thickness, with notable success (Fichefet et al., 2003; Losh et al., 2010; Timmermann and Beckmann, 2004; Timmermann et al., 2002, 2004, 2005, 2009).

2. Objectives

The objective of the present study is to assess the appropriateness of MITgcm model derived monthly average sea ice concentration (and hence sea ice area) for sea ice monitoring over Arctic region. Hence, Sea Ice Area (SIA) calculated from model simulated Sea Ice Concentration (SIC) from 1980 to 2010 has been compared with SIA available from satellite data.

3. Study area and data used

The study area for this study covers Arctic region where sea ice is available. The MITgcm simulated mean monthly SIC values at 1^0 x 1^0 grid were used for calculating monthly averaged SIA from 1980 to 2010. Satellite derived SIA from 1979 to 2013 were obtained from ftp://sidads.colorado.edu/DATASETS/NOAA/G02135 (Fetterer et al., 2002). The monthly SIA data were calculated from daily SIC values. The SIC values were estimated using passive microwave satellite data i.e. Scanning Multichannel Microwave Radiometer (SMMR), Special Sensor Microwave/Imager (SSM/I), Special Sensor Microwave Imager/Sounder (SSMIS). More information on satellite derived SIA data is available at http://nsidc.org/data/g02135.html.

4. MITgcm model simulations for sea ice

In the current study, we use the Massachusetts Institute of Technology General Circulation Model (MITgcm, Marshall et al., 1997) which is a general circulation ocean model with a sea-ice model included in it. This model has a provision to run both the ocean and ice

model in an interactive mode. The model is widely used and has an active user community for all sorts of ocean ice problems. MITgcm Version checkpoint62b has been used in this study; (The manual can be accessed from this link http://mitgcm.org/public/r2_manual/latest/online_documents/node2.html). In order to identify the contribution of thermodynamic process individually, for this particular study the sea-ice dynamics was kept disabled and ice melting and evolution was due to thermodynamic processes alone (Zhang and Hibler, 1997).

The zonal grid spacing is 1° longitude, while the meridional ocean grid spacing is 0.3° of latitude within 10° of the Equator increasing to 1° latitude pole-ward of 22°N and 22°S. . This is done to better capture the equatorial ocean variability. In order to avoid singularity at the North Pole, the model last grid point in latitude is of 4° resolution, i.e. after 86°N we have the northernmost point 90° N. Additionally zonal filter has been applied to filter out fast gravity waves at the poles. In the vertical direction there are 46 ocean levels with thicknesses ranging from 10 m in the top 150 m, and gradually increasing to 400 m thickness near the maximum model depth of 5815 m. The model's bathymetry is based on ETOPO5 (Data Announcement 88MGG-02, Digital relief of the Surface of the Earth, NOAA, National Geophysical Data Centre, Boulder, Colorado, 1988). The OGCM employs the K-Profile Parameterization (KPP) vertical mixing scheme of Large et al. (1994) and the isopycnal mixing schemes of Redi (1982) and Gent and McWilliams (1990) with surface tapering as per Large et al. (1997).

Laplacian diffusion and friction are used except that horizontal friction is bi-harmonic. Isopycnal diffusivity and isopycnal thickness diffusivity is 500 m^2s^{-1}. Vertical diffusivity is 5 x 10^{-6} m^2s^{-1}. Horizontal and vertical viscosities are 1013 m^2s^{-1} and 10^{-4} m^2s^{-1}, respectively. No-slip bottom, free-slip lateral, and free surface boundary conditions are employed. The model is initialized using climatological temperature and salinity for the month of January from Levitus et al. (1994) and is integrated forward in time under cold start conditions (u, v = 0).

The 6-hourly forcing fields of 2m air temperature, specific humidity, net surface solar radiation, downward long-wave radiation, 10m zonal and meridional winds and surface net precipitation have been taken from NCEP reanalysis (Kalnay 1996) The model is integrated starting from 1948 until 2010 and the output is stored on a monthly basis. For analysis purpose we use the model results starting from 1980 onwards.

5. Results and discussion

Model Simulated Mean Monthly SIA (MSMMSIA) variations with year (1980 to 2010) over Arctic region clearly show that SIA during winter months (January, February, March, April) are high while during summer months (July, August, September, October) are low. The SIA values during May, June, November and December months are between these two extremes (Fig 1). This behaviour is similar to that observed through satellite data analysis. Mean sea ice growth cycle (melting during summer and refreezing during winter) plot prepared from 31-year averaged monthly MSMMSIA data is presented in Fig 2. The median values which are very close to mean values are also plotted. Overall long term decreasing trend of MSMMSIA is shown in Fig 3. A linear trend fitted to 31-year mean annual SIA data resulted in following equation –

Model Mean Annual SIA = - 0.037 x Year +83.08
(R^2=0.67, SEOE= 0.24, F value=58.3, P value < 0.001)

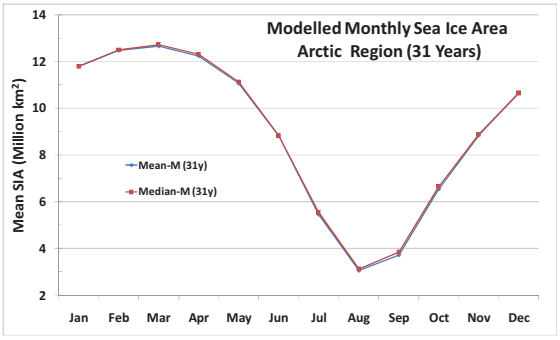

Figure 2: Sea ice melt and refreezing cycle over Arctic region

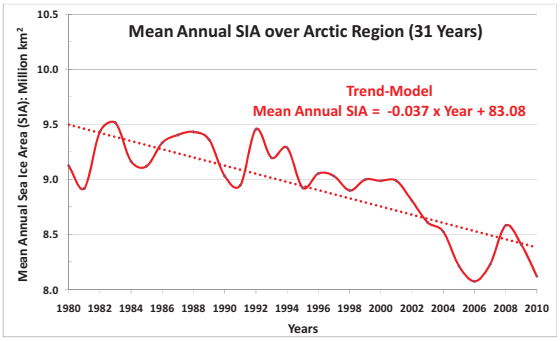

Figure 3: Long term decreasing trend from MSMMSIA over Arctic region

The linear trend is found statistically significant at 99% confidence level. Negative value of the coefficient (-0.037) shows that there is a decreasing trend in SIA values during this period.

It is found that the general patterns of sea ice growth cycles derived from MSMMSIA data over Arctic region are similar to that obtained from Satellite Derived Mean Monthly SIA (SDMMSIA) data for the same time period (Fig 4). In Arctic region, MSMMSIA values are mostly lower than SDMMSIA values especially during peak summer and peak winter period in northern hemisphere. It shows that MITgcm is underestimating SIA during peaks of summer and winter in Arctic region.

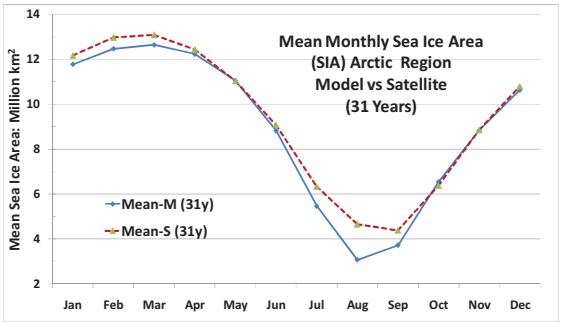

Figure 4: Comparison sea ice cycles from MSMMSIA and SDMMSIA over Arctic region

The linear trends fitted for MSMMSIA and SDMMSIA values are shown in Fig 5. Both the trends show that SIA is decreasing in Arctic region with time during this period; the rate of decrease is overestimated by MITgcm.

There is high correlation (coefficient of correlation = 0.75) between MSMMSIA and SDMMSIA values. The relative deviations (RD) between model and satellite based SIA ranges from -8.3% (during 2004) to 2.6% (during 1984) with average RD being -4.2%. While the model suggests SIA decrease of 3.7% in 31-year period; satellite observed only 1.8% decrease during this period.

Satellite Mean Annual SIA = - 0.018 x Year + 45.19
(R^2=0.17, SEOE= 0.37, F value=5.9, P value = 0.021)

The above trend is statistically significant at 95% confidence level. A close observation of SDMMSIA variations with year clearly shows that there was an increasing trend in from 1980 to 1992 period which has not been picked up in the model simulated SIA values (see Fig 5).

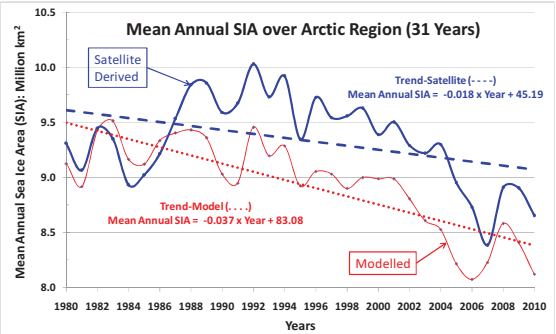

Figure 5: Comparison sea ice trends from MSMMSIA and SDMMSIA over Arctic region

Hence, two part analysis of SDMMSIA data was carried out for 1979 to 2013 period (Fig 6). Following are the three linear trends obtained from this analysis –

Period 1979 – 1992:
Mean Annual SIA = 0.054 x Year - 98.80
(R^2=0.47, SEOE= 0.25, F value=10.8, P value = 0.006)

Period 1993 - 2013:
Mean Annual SIA = -0.068 x Year + 146.9
(R^2=0.80, SEOE= 0.21, F value=79.1, P value < 0.001)

Period 1979 - 2013:
Mean Annual SIA = -0.023 x Year + 55.58
(R^2=0.29, SEOE= 0.37, F value=13.4, P value < 0.001)

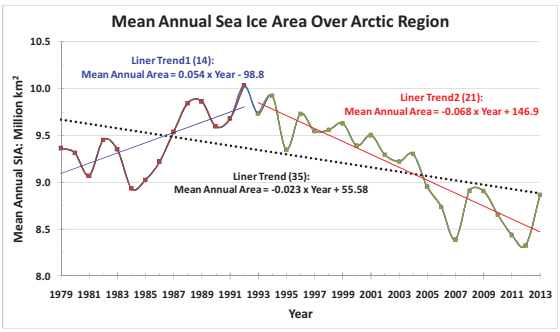

Figure 6: Reversal of sea ice trends from 1992 as per SDMMSIA (1979-2013) data over Arctic region

It shows that there was an increase of 5.4% SIA from 1979 to 1992 period followed by a decrease of 6.8% from 1993 to 2013 period. It resulted in an overall decrease of 2.3% in SIA between 1979 and 2013 in Arctic region. All the three linear trends were found statistically significant at 99% confidence level.

6. Conclusions

Sea ice concentration (SIC) over Arctic region was simulated with MIT global circulation model (MITgcm) from 1980 to 2010. The inputs were acquired from various sources and output SIC was available at 1^o x 1^o over Arctic Regions. Sea ice area calculated from SIC and grid geographic area was compared with satellite derived NSIDC/NASATEAM sea ice area. In the Arctic region, simulated sea ice area trends were quite similar to satellite derived sea ice area trends. In model overestimated the rate of decrease of sea ice area when compared to satellite derived sea ice area. An important temporal phenomenon has been observed while analysing mean monthly satellite derived sea ice area. It was found that sea ice area initially increased during 1979 to 1992 time period by 5.4% followed by a reduction of 6.8% between 1993 and 2013 time period. Overall, a decrease of almost 2.3% has been observed from 1979 to 2013.

A more detailed study requires to be carried out by incorporating sea ice dynamics into MITgcm model. There is a need to find out the cause of observed sea ice trend reversal 1993 onward, in Arctic. We also need to assimilate satellite derived SIC in the model to correct for the model bias.

Acknowledgements

The authors sincerely thank Director SAC, Shri Tapan Misra for his constant encouragement provided during

this study. We thank Deputy Director EPSA, Dr. Pradip Pal and Group Director AOSG, Dr. Raj Kumar for their guidance and support at all stages of the study. We herewith acknowledge that the sea ice area (1979 to 2013) data used in this study were downloaded from following two sites, respectively (1) ftp://sidads.colorado.edu/DATASETS/NOAA/G02135 and (2) ftp://sidads.colorado.edu/pub/DATASETS/nsidc0081_nrt_nasateam_seaice/

NCEP 6 hourly forcing fields were taken from http://www.esrl.noaa.gov/psd/data/gridded/data.ncep.reanalysis.surfaceflux.html.

References

Bitz, C.M. and W.H. Lipscomb (1999).An energy-conserving thermodynamic model of sea ice. Journal of Geophysical Research, 104, 15669-15677.

Budyko, M.I. (1969). The effect of solar radiatin variations on the climate of the earth.Tellus, 21, 611–619.

Breivik, L.A., S. Eastwood, Ø. Godøy, H. Schyberg, S. Andersen and R.T. Tonboe (2014). Sea ice products for EUMETSAT satellite application facility. Canadian Journal of Remote Sensing, 27 (5), 403-410. DOI: 10.1080/07038992.2001.10854883.

Cavalieri, D.J., P. Gloersen and W.J. Campbell (1984). Determination of sea ice parameters with the Nimbus7 SMMR. J. Geophys. Res., 89, 5355-5369.

Cavalieri, D.J., C.L. Parkinson, P. Gloersen and H. Zwally (1996). Updated yearly.Sea ice concentrations from Nimbus-7 SMMR and DMSP SSM/I-SSMIS passive microwave data. [1979 to 2013]. Boulder, Colorado USA: NASA DAAC at the National Snow and Ice Data Center.

Comiso, J.C. (1986). Characteristics of Arctic winter sea ice from satellite multispectral microwave observations. Journal of Geophysical Research, 91, 975-994.

Comiso, J.C. (1995). SSM/I concentrations using the bootstrap algorithm.NASA Report, 1380.

Fetterer, F., K. Knowles, W. Meier and M. Savoie (2002). Sea Ice Index. [Sea Ice Area, used from 1980 to 2010]. Boulder, Colorado USA: National Snow and Ice Data Center. http://dx.doi.org/10.7265/N5QJ7F7W.

Fichefet, T., B. Tartinville and H. Goosse (2003). Antarctic sea ice variability during 1958–1999: A simulation with a global ice-ocean model. J. Geophys. Res., 108 (C3), 3102, doi:10.1029/2001JC001148.

Gent, P.R. and J.C. McWilliams (1990). Isopycnal mixing in ocean circulation models. J. Phys. Oceanogr., 20:150-155.

Gloersen, P., W.J. Campbell, D.J. Cavalieri, J.C. Comiso, C.L. Parkinson and H.J. Zwally (1992). Arctic and Antarctic sea ice, 1978–1987.Satellite passive-microwave observations and analysis.NASA SP-511. Washington, D.C.: National Aeronautics and Space Administration.

Hellmer, H.H. (2004). Impact of Antarctic ice shelf basal melting on sea ice and deep ocean properties.Geophys. Res. Lett., 31,L10307, doi:10.1029/2004GL019506

Hibler, W.D. (1979). A dynamic thermodynamic sea ice model. J. Phys. Oceanogr., 9, 815–846.

Hibler, W.D. (1980). Modeling a variable thickness sea ice cover. Mon. Wea. Rev., 108:1943-1973.

Hunke, E.C. and J.K. Dukowicz (1997). An elastic-viscous-plastic model for sea ice dynamics. J. Phys. Oceanogr., 27, 1849–1867.

Kaleschke, L., G. Heygster, C. Lüpkes, A. Bochert, J. Hartmann, J. Haarpaintner and T. Vihma (2001). SSM/I sea ice remote sensing for mesoscale ocean-atmosphere interaction analysis. Canadian Journal of Remote Sensing, 27, 526–537.

Kalnay, E., M. Kanamitsu, R. Kistler, W. Collins, D. Deaven, L. Gandin, M. Ireden, S. Saha, G. White, J. Woollen, Y. Zhu, A. Leetmaa, R. Reynolds, M. Chelliah, W. Ebisuzaki, W. Higgins, J. Janowiak, K.C. Mo, C. Ropelewski, J. Wang, R. Jenne, and D. Joseph (1996). The NCEP/NCAR 40 year reanalysis project. Bulletin of Am. Met. Society 77, 437–471.

Large, W.G., G. Danabasoglu, S.C. Doney and J.C. McWilliams (1997). Sensitivity to surface forcing and boundary layer mixing in a global ocean model: Annual-mean climatology. J. Phys. Oceanogr., 27, 2418-2447

Large, W.G., J.C. McWilliams and S.C. Doney (1994). Oceanic vertical mixing: A review and a model with a nonlocal boundary layer parameterization. Rev Geophys, 32, 363-403

Lefebvre, W. and H. Goosse (2005). Influence of the southern annular mode on the sea ice-ocean system: The role of the thermal and mechanical forcing. Ocean Sci., 1, 145–157, doi:10.5194/os-1-145-2005.

Lefebvre, W. and H. Goosse (2008). An analysis of the atmospheric processes driving the large-scale winter sea ice variability in the Southern Ocean. J. Geophys. Res., 113, C02004, doi:10.1029/2006JC004032

Levitus, S., T. Boyer and J. Antonov (1994). World Ocean Atlas 1994, Vol. 5: Interannual variability of upper ocean thermal structure. NOAA Atlas NESDIS 5. U.S. Gov. Printing Office, Wash., D.C., 176 pp.

Losh, M., D. Menemenlis, J.M. Campin, P. Heimbach and C. Hillm (2010). On the formulation of sea-ice models. Part 1: Effects of different solver implementations and parameterizations. Ocean Model., 33, 129–144, doi:10.1016/j.ocemod.2009.12.008

Markus, T. and D. Cavalieri (2000). An enhancement of the NASA team sea ice algorithm. IEEE Transactions on Geoscience and Remote Sensing, 38, 1387-1398.

Marshall, J., A. Adcroft, C. Hill, L. Perelman and C. Heisey (1997). A finite-volume, incompressible Navier–Stokes model for studies of the ocean on parallel computers. J. Geophys. Res., 102, 5753–5766, doi:10.1029/96JC02775.

Massom, R.A., Hajo E., Christian H., Martin O.J., Drinkwater M.R., Matthew S., Anthony P.W., Wu X., Victoria I.L., Shuki U., Morris K., Reid P.A., Warren S.G., and A. Ian (2001). Snow on Antarctic sea ice. Reviews of Geophysics , 39(3):413-445. DOI:10.1029/2000RG000085.

Maykut, G.A. and N. Untersteiner (1971). Some results from a time-dependent thermodynamic model of sea ice. J. Geophys. Res., 76, 1550–1575.

Oza, S,R., R.K.K. Singh, N.K. Vyas and A. Sarkar (2010). Recent trends of Arctic and Antarctic summer sea-ice cover observed from space-borne scatterometer. J. Indian Soc Remote Sens, 38(4):611–616. DOI 10.1007/s12524-011-0071-9.

Powell, D.C., T. Markus and A. Stossel (2005). Effects of snow depth forcing on Southern Ocean sea ice simulations. J. Geophys. Res., 110, C06001, doi:10.1029/2003JC002212.

Redi, M.H. (1982). Oceanic isopycanal mixing by coordinate rotation. J. Phys. Oceanogr., 12:1154–1158. Sellers, W.D. (1969).A global climate model based on the energy balance of the earth-atmosphere system. J. Appl. Meteor., 8, 392–400.

Shalina, E.V. and O.M. Johannessen (2008). Multi year sea ice concentration mapping using passive and active microwave satellite data. Microwave Radiometry and Remote Sensing of the Environment-MICRORAD 2008, 1-4, doi: 10.1109/MICRAD.2008.4579513.

Spreen, G., L. Kaleschke and G. Heygster (2008). Sea ice remote sensing using AMSR-E 89 GHz channels. Journal of Geophysical Research, 113, doi:10.1029/2007GL032461.

Stossel, A., Z.R. Zhang, and T. Vihma (2011). The effect of alternative real-time wind forcing on Southern Ocean sea icesimulations. J. Geophys. Res., 116, C11021, doi:10.1029/2011JC007328.

Timmermann, R. and A. Beckmann (2004). Parameterization of vertical mixing in the Weddell sea. Ocean Modell., 6, 83–100,doi:10.1016/S1463-5003(02)00061-6.

Timmermann, R., A. Beckmann and H.H. Hellmer (2002). Simulations of ice-ocean dynamics in the Weddell Sea 1.Model configuration and validation. J. Geophys. Res., 107 (C3), doi:10.1029/2000JC000741

Timmermann, R., A. Worby, H. Goosse and T. Fichefet (2004). Utilizing the ASPeCt sea ice thickness data set to evaluate a global coupledsea ice-ocean model. J. Geophys. Res., 109, C07017, doi:10.1029/2003JC002242.

Timmermann, R., H. Goosse, G. Madec, T. Fichefet, C. Ethe, and V. Duliere (2005). On the representation of high latitude processes in theORCA-LIM global coupled sea ice-ocean model. Ocean Modell., 8, 175–201, doi:10.1016/j.ocemod.2003.12.009.

Timmermann, R., S. Danilov, J. Schroter, C. Boning, D. Sidorenko, and K. Rollenhagen (2009). Ocean circulation and sea ice distribution in a finite element global sea ice-ocean model. Ocean Modell., 27, 114–129, doi:10.1016/j.ocemod.2008.10.009.

Walker, N.P., Partington, K.C., Van Woert, M.L., and Street, L.T. (2006). Arctic sea ice type and concentration mapping using passive and active microwave sensors. IEEE Transactions Geoscience Remote Sensing, 44 (12), 3574-3584.

Zhang, J. and W.D. Hibler III (1997). On an efficient numerical method for modeling sea ice dynamics. J. Geophys. Res., 102,8691–8702.

Zwally, J.H., Donghui Yi, Ron Kwok and Yunhe Zhao (2008). ICESat measurements of sea ice freeboard and estimates of sea ice thickness in the Weddell Sea. J. Geophys. Res. 113 (C02S15). doi:10.1029/2007JC004284.